Vol 18 No 4, April 2009
1674-1056/2009/18(04)/1322-06

Chinese Physics B

© 2009 Chin. Phys. Soc.
and IOP Publishing Ltd

Lattice models of traffic flow considering drivers' delay in response*

Zhu Hui-Bing(祝会兵)†

Faculty of Architectural, Civil Engineering and Environment, Ningbo University, Ningbo 315211, *China*

(Received 24 July 2008; revised manuscript received 2 September 2008)

This paper proposes two lattice traffic models by taking into account the drivers' delay in response. The lattice versions of the hydrodynamic model are described by the differential-difference equation and difference-difference equation, respectively. The stability conditions for the two models are obtained by using the linear stability theory. The modified KdV equation near the critical point is derived to describe the traffic jam by using the reductive perturbation method, and the kink–antikink soliton solutions related to the traffic density waves are obtained. The results show that the drivers' delay in sensing headway plays an important role in jamming transition.

Keywords: lattice hydrodynamic model, traffic jams, analytical method, drivers' delay in response
PACC: 0340K, 0570F, 0570J

1. Introduction

Traffic jams have attracted much attention and have been studied by various traffic models: car following models, cellular automaton models, gas kinetic models, and hydrodynamic models.[1−18] The hydrodynamic models and car following models have been studied analytically by the linear stability theory and the nonlinear analysis method. Kurtze and Hong[6] have derived the Korteweg-de Vries (KdV) equation from the hydrodynamic model.[7] They have shown that the traffic soliton appears near the neutral stability line. Komatsu and Sasa[8] have derived the modified KdV (mKdV) equation from the optimal velocity model (a car following model). They have shown that the traffic jam is described in terms of a kink density wave near the critical point.

Recently, the lattice hydrodynamic models have been developed quickly after the first lattice version of continuum model was proposed at 1998 by Nagatani.[9] He presented two hydrodynamic models to describe the jamming transition on a single lane highway. One is a simplified version of continuum model described in terms of the partial differential equations and the other is the lattice version given by the difference equations. The mKdV equation near the critical point was also derived by using the reduction perturbation method.

The first model is described as

$$\partial_t \rho + \partial_x(\rho v) = 0, \tag{1}$$

$$\partial_t(\rho v) = a\rho_0 V(\rho(x+h_0)) - a\rho v, \tag{2}$$

where ρ_0 is the average density, and a is the sensitivity of a driver, h_0 represents the average headway, $h_0 = 1/\rho_0$, $\rho(x+h_0)$ is the local density at position $x+h_0$ at time t, which is related with the inverse of headway $h(x,t)$, i.e. $\rho(x+h_0) = 1/h(x,t)$. The idea is that a driver adjusts the vehicle velocity according to the observed headway $h(x,t)$ or density ahead $\rho(x+h_0)$.

The lattice version of the model with dimensionless space x is described as

$$\partial_t \rho_j + \rho_0(\rho_j v_j - \rho_{j-1} v_{j-1}) = 0, \tag{3}$$

$$\partial_t \rho_j v_j = a\rho_0 V(\rho_{j+1}) - a\rho_j v_j, \tag{4}$$

where j denotes the site on the one-dimensional lattice, and ρ_j, v_j denote the local density and the local average velocity on site j at time t, respectively.

Then Nagatani proposed another simple lattice model.[10] Xue proposed a lattice model of optimal

*Project supported by the National Basic Research Program of China (Grant No 2006CB705500), the National Natural Science Foundation of China (Grant No 10532060), the Natural Science Foundation of Ningbo (Grant Nos 2008A610022 and 2007A610050), and K. C. Wang Magna Fund in Ningbo University, China.
†Corresponding author. E-mail: zhuhuibing@nbu.edu.cn

traffic flow considering the optimal current of the next-nearest-neighbour interaction.[11] Ge *et al* proposed an extended lattice model considering an arbitrary number of sites ahead on a single-lane highway.[12] Further the models were applied to investigate jamming transition and critical phenomenon on a two-lane highway and in high-dimensional traffic flow.[13,14]

However all these models adopt the optimal velocity function which is dependent on the observed headway at time t. But in reality a driver makes up his mind to accelerate or not after he senses the headway. That is to say, a driver senses headway at time t and makes a decision to change the velocity of his car at later time $t+\tau_1$, in which τ_1 is the delay of the drivers' response in sensing headway and reflected in the optimal velocity. Then the vehicle moves at time $t+\tau_1+\tau_2$, where τ_2 is the delay of car motion.

In this paper, we present two extended versions of continuum models of traffic which take into account the drivers' delay in sensing headway and the delay of car motion respectively. We apply the linear stability theory and the nonlinear analysis method to the two models and obtain the neutral stability lines and the mKdV equations.

The organization of this paper is as follows. In Section 2 two continuum traffic models are proposed by taking into account the drivers' delay in sensing headway in the optimal velocity function. In Section 3 the stability of uniform traffic flow is analysed by the linear stability theory, and the neutral stability line and the critical point are obtained. In Section 4 the mKdV equation around the critical point is derived by applying the reductive perturbation method. In Section 5 the result of analysis is presented. Section 6 gives a summary.

2. Models

The two extended lattice versions of the continuum models are proposed, which take into account the drivers' delay in sensing headway and the delay of car motion respectively. They are called models A and B:

$$\partial_t \rho_j + \rho_0(\rho_j v_j - \rho_{j-1} v_{j-1}) = 0, \tag{5}$$

$$\begin{aligned} &\rho_j(t+\tau)v_j(t+\tau) \\ &= \rho_0 V(\rho_{j+1}(t-n\tau)), \quad \text{for model A} \end{aligned} \tag{6}$$

$$\begin{aligned} &\rho_j(t+\tau) - \rho_j(t) + \tau\rho_0\rho_j(t)v_j(t) \\ &-\tau\rho_0\rho_{j-1}(t)v_{j-1}(t) = 0, \end{aligned} \tag{7}$$

$$\begin{aligned} &\rho_j(t+\tau)v_j(t+\tau) \\ &= \rho_0 V(\rho_{j+1}(t-n\tau)), \quad \text{for model B.} \end{aligned} \tag{8}$$

The optimal velocity V is selected in a way similar to that proposed by Bando *et al*,[15]

$$\begin{aligned} &V(h_j(t-n\tau)) \\ &= \frac{v_{\max}}{2}[\tanh(h_j(t-n\tau)-h_c)+\tanh(h_c)]. \end{aligned} \tag{9}$$

It can be expressed as another form similar to that in Ref.[9],

$$\begin{aligned} &V(\rho_j(t-n\tau)) \\ &= \frac{v_{\max}}{2}\left[\tanh\left(\frac{1}{\rho_j(t-n\tau)}-h_c\right)+\tanh(h_c)\right], \end{aligned} \tag{10}$$

where $v_{\max}$ is the maximal velocity of vehicles (for simplicity, $v_{\max}=2$), and h_c is the safety distance of vehicles. When the headway is less than the safety distance, the vehicle reduces its velocity to prevent from crashing into the preceding vehicle. On the other hand, if the headway is larger than the safety distance, the vehicle increases its velocity to the maximum velocity. The reason we choose the form of Bando *et al*, other than that of Whitham,[16] lies in the fact that the former is a monotonically increasing function with an upper bound (maximal velocity) and has a turning point (inflection point) at $h_j = h_c$: $V''(h_c) = 0$. This property is important for us to derive the mKdV equation which gives traffic jams in terms of a kink density wave.

In the models, the total delay time is divided into two parts, one is the drivers' delay in sensing headway and another is the delay time of car motion. For simplicity, τ denotes the total delay time, and $n\tau$ denotes the drivers' delay in response in our models, in which n is a parameter denoting the relationship between the drivers' delay and the total delay. We take the value of n as $0, 0.1, 0.2, 0.3$ on account of the fact that the delay time of car motion is of the order of 1 sec, and the known physical or mechanical response time is of the order of 0.1 sec.[17] The sensitivity a equals the inverse of the total delay time, i.e. $a = 1/\tau$.

By eliminating velocity term in Eqs.(5) and (6) [and also in Eqs.(7) and (8)], we obtain the density equations for models A and B:

$$\begin{aligned} &\partial_t \rho_j(t+\tau) + \rho_0^2[V(\rho_{j+1}(t-n\tau)) \\ &-V(\rho_j(t-n\tau))] = 0, \end{aligned} \tag{11}$$

$$\begin{aligned} &\rho_j(t+2\tau) - \rho_j(t+\tau) + \tau\rho_0^2[V(\rho_{j+1}(t-n\tau)) \\ &-V(\rho_j(t-n\tau))] = 0. \end{aligned} \tag{12}$$

In the limit case of $n = 0$, equations (11) and (12) reduce to the density equation of the original lattice hydrodynamic models.[10]

3. Linear stability analysis

The linear stability analysis is conducted for the above extended lattice models. It is obvious that the uniform traffic flow with constant density ρ_0 and constant optimal velocity $V(\rho_0)$ is the steady-state solution for Eqs.(11) and (12), which is given as:

$$\rho_j(t) = \rho_0 \quad \text{and} \quad v_j = V(\rho_0). \tag{13}$$

Suppose that $y_j(t)$ is a small deviation from the steady-state density of the j-th vehicle,

$$\rho_j(t) = \rho_0 + y_j. \tag{14}$$

Substituting Eq.(14) into Eqs.(11) and (12) and linearizing them, we get the resultant equations:

$$\begin{aligned}&\partial_t y_j(t+\tau) + \rho_0^2 V'(\rho_0)[y_{j+1}(t-n\tau)\\ &-y_j(t-n\tau)] = 0,\end{aligned} \tag{15}$$

$$\begin{aligned}&y_j(t+2\tau) - y_j(t+\tau) + \tau\rho_0^2 V'(\rho_0)[y_{j+1}(t-n\tau)\\ &-y_j(t-n\tau)] = 0,\end{aligned} \tag{16}$$

where $V'(\rho_0) = \mathrm{d}V(\rho_j)/\mathrm{d}\rho_j \mid_{\rho_j=\rho_0}$. For simplicity, $V'(\rho_0)$ is indicated as V' hereafter.

Expanding y_j in the Fourier modes: $y_j(t) = \exp(\mathrm{i}kj + zt)$, where $z = z_1(\mathrm{i}k) + z_2(\mathrm{i}k)^2 + \ldots$, and inserting them into Eqs.(15) and (16), then we can get the first- and second-order terms of coefficients in the expression of z respectively as follows:

$$\begin{aligned}&z_1 = -\rho_0^2 V' \quad \text{and}\\ &z_2 = -\frac{\rho_0^2 V'}{2} - (n+1)\tau(\rho_0^2 V')^2,\end{aligned} \tag{17}$$

$$\begin{aligned}&z_1 = -\rho_0^2 V' \quad \text{and}\\ &z_2 = -\frac{\rho_0^2 V'}{2} - (n+\frac{3}{2})\tau(\rho_0^2 V')^2.\end{aligned} \tag{18}$$

Thus the neutral stability condition is given by

$$\tau = -\frac{1}{2(n+1)\rho_0^2 V'} \qquad \text{for model A,} \tag{19}$$

$$\tau = -\frac{1}{(2n+3)\rho_0^2 V'} \qquad \text{for model B.} \tag{20}$$

For small disturbances with long wavelengths, the uniform traffic flow is unstable when the following condition is satisfied:

$$\tau > -\frac{1}{2(n+1)\rho_0^2 V'} \qquad \text{for model A,} \tag{21}$$

$$\tau > -\frac{1}{(2n+3)\rho_0^2 V'} \qquad \text{for model B.} \tag{22}$$

4. Nonlinear analysis

We apply the reductive perturbation method to Eqs.(11) and (12) focusing on the system behaviour near the critical point (ρ_c, a_c). Then the nature of kink–antikink soliton solutions can be described by the mKdV equation. We introduce slow scales for space variable j and time variable t, and define the slow variables X and T as:

$$X = \varepsilon(j + bt), \quad T = \varepsilon^3 t, \quad 0 < \varepsilon \ll 1, \tag{23}$$

where b is a constant to be determined. Let

$$\rho_j(t) = \rho_c + \varepsilon R(X, T). \tag{24}$$

Substituting Eqs.(23) and (24) into Eqs.(11), (12) and making the Taylor expansions to the fifth order of ε, we obtain the following expression (see Appendix)

$$\begin{aligned}&\varepsilon^2(b+\rho_c^2 V')\partial_X R + \varepsilon^3\left[b^2\tau + \left(\frac{1}{2} - bn\tau\right)\rho_c^2 V'\right]\partial_X^2 R\\ &+\varepsilon^4\left[\partial_T R + \left(b^3\tau^2/2 + \left(\frac{1}{6} - bn\tau/2 + b^2n^2\tau^2/2\right)\rho_c^2 V'\right)\partial_X^3 R + \frac{1}{6}\rho_c^2 V'''\partial_X R^3\right]\\ &+\varepsilon^5[(2b\tau - n\tau\rho_c^2 V')\partial_X\partial_T R + (b^4\tau^3/6 + (1/24 - bn\tau/6 + b^2n^2\tau^2/4\\ &-b^3n^3\tau^3/6)\rho_c^2 V')\partial_X^4 R + \frac{1}{6}\rho_c^2 V'''(1/2 - bn\tau)\partial_X^2 R^3] = 0,\end{aligned} \tag{25}$$

$$\varepsilon^2(b+\rho_c^2 V')\partial_X R + \varepsilon^3\left[3b^2\tau/2 + \left(\frac{1}{2} - bn\tau\right)\rho_c^2 V'\right]\partial_X^2 R + \varepsilon^4\Big[\partial_T R$$

$$+\left(7b^3\tau^2/6+\left(\frac{1}{6}-bn\tau/2+b^2n^2\tau^2/2\right)\rho_c^2V'\right)\partial_X^3R+\frac{1}{6}\rho_c^2V'''\partial_XR^3\Big]$$
$$+\varepsilon^5\Big[(3b\tau-n\tau\rho_c^2V')\partial_X\partial_TR+(5b^4\tau^3/8+(1/24-bn\tau/6+b^2n^2\tau^2/4$$
$$-b^3n^3\tau^3/6)\rho_c^2V')\partial_X^4R+\frac{1}{6}\rho_c^2V'''(1/2-bn\tau)\partial_X^2R^3\Big]=0, \quad (26)$$

where $V'=\left.\frac{\mathrm{d}V(\rho_j)}{\mathrm{d}\rho_j}\right|_{\rho_j=\rho_c}$ and $V'''=\left.\frac{\mathrm{d}^3V(\rho_j)}{\mathrm{d}\rho_j^3}\right|_{\rho_j=\rho_c}$. V' and V''' correspond to $V'(\rho_c)$, $V'''(\rho_c)$ in the above equation and hereafter. Near the critical point (ρ_c,a_c), $\tau=(1+\varepsilon^2)\tau_c$ or $a=a_c(1-\varepsilon^2)$. By taking $b=-\rho_c^2V'(h_c)$ and eliminating the second- and third-order terms of ε from Eqs.(25) and (26), we obtain the simplified equation:

$$\varepsilon^4[\partial_TR-g_1\partial_X^3R+g_2\partial_XR^3]$$
$$+\varepsilon^5[g_3\partial_X^2R+g_4\partial_X^4R+g_5\partial_X^2R^3]=0, \quad (27)$$

where $g_1=-\rho_c^2V'/24$, $g_2=\rho_c^2V'''/6$, $g_3=-\rho_c^2V'/2$, $g_4=-\rho_c^2V'/48$, $g_5=-\rho_c^2V'''/12$ for Eq.(25), and $g_1=\frac{n^2+3n+2}{6(2n+3)^2}\rho_c^2V'$, $g_2=\rho_c^2V'''/6$, $g_3=-\rho_c^2V'/2$, $g_4=-\frac{n^2+3n+2}{12(2n+3)^2}\rho_c^2V'$, $g_5=-\rho_c^2V'''/12$ for Eq.(26).

In order to obtain the standard mKdV equation with higher order correction, we make the following transformations for Eq.(27):

$$T=\frac{1}{g_1}T', \quad R=\sqrt{\frac{g_1}{g_2}}R'. \quad (28)$$

Then we have the following standard mKdV equation with an $O(\varepsilon)$ correction term:

$$\partial_{T'}R'-\partial_X^3R'+\partial_XR'^3$$
$$+\frac{\varepsilon}{g_1}\left[g_3\partial_X^2R'+g_4\partial_X^4R'+\frac{g_1g_5}{g_2}\partial_X^2R'^3\right]=0. \quad (29)$$

We ignore the $O(\varepsilon)$ term in Eq.(29), and get the mKdV equation with the kink–antikink soliton solution:

$$R_0'(X,T')=\sqrt{c}\tanh\sqrt{\frac{c}{2}}(X-cT'). \quad (30)$$

Next, we take into account the $O(\varepsilon)$ term and suppose $R'(X,T')=R_0'(X,T')+\varepsilon R_1'(X,T')$. We obtain the selected velocity c and adopt the following expression according to Ref.[18]:

$$c=\frac{5g_2g_3}{2g_2g_4-3g_1g_5}. \quad (31)$$

Thus the following general kink–antikink soliton solution for models A and B, i.e., the mKdV equation, is obtained:

$$\rho_j(t)=\rho_c\pm\sqrt{\frac{-6\rho_c^2V'}{\rho_c^2V'''}(\tau/\tau_c-1)}$$
$$\times\tanh\left[\sqrt{\frac{c}{2}(\tau/\tau_c-1)}\right.$$
$$\left.\times\{j-(1-\sqrt{\tau/\tau_c-1})\rho_c^2V't\}\right], \quad (32)$$

where $c=24$, $\tau_c=-1/2(n+1)\rho_c^2V'$ for model A, and $c=\frac{6(2n+3)^2}{n^2+3n+2}$, $\tau_c=-1/(2n+3)\rho_c^2V'$ for model B.

Then we obtain the coexisting curves in terms of the original parameters:

$$\rho_{co}=\rho_c\pm\sqrt{\frac{-6\rho_c^2V'[-2(n+1)\rho_c^2V'\tau-1]}{\rho_c^2V'''}}$$
for model A, (33)

$$\rho_{co}=\rho_c\pm\sqrt{\frac{-6\rho_c^2V'[-(2n+3)\rho_c^2V'\tau-1]}{\rho_c^2V'''}}$$
for model B. (34)

5. Result of analysis and discussion

Figure 1 shows the relationship between the headway $h=1/\rho$ and the sensitivity $a=1/\tau$ with $h_c=4.0$, $-\rho_c^2V'=1$ and $\rho_c^2V'''=2$ given in Eq.(9). There are two clusters of curves and they correspond to models A and B respectively. In each cluster of diagram, there are four pairs of curves corresponding to the situation of $n=0,0.1,0.2,0.3$ from the bottom to the top respectively. The corresponding critical points, the neutral stability lines and the coexisting curves in model A are lower than those in model B. Each dotted curve indicates the coexisting curve given by Eqs.(33) and (34) for models A and B respectively. Each solid line indicates the neutral stability line given by Eqs.(19) and (20) for models A and B respectively. The apexes of lines correspond to the critical points and expressed as $(h_c,a_c)=[h_c,-2(n+1)\rho_c^2V'(h_c)]$

for model A and $(h_c, a_c) = [h_c, -(2n+3)\rho_c^2 V'(h_c)]$ for model B.

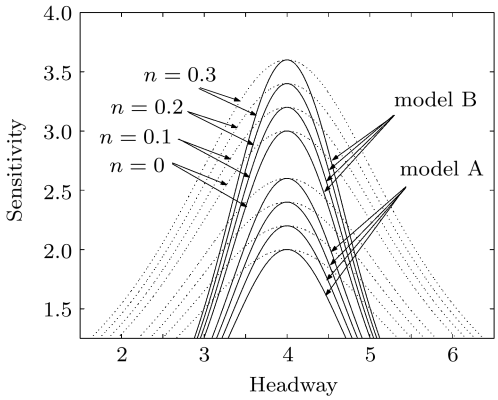


Fig.1. The diagram in the headway-sensitivity space considering different delay of drivers' response in sensing headway for models A and B.

In the region outside the coexisting curve, the freely moving phase exists. The intermediate region between the coexisting curve and the neutral stability line represents the metastable region. And the region inside the neutral stability line represents the congested phase. It can be seen that when we take into account the drivers' delay in response, the critical sensitivity a_c will increase with the increase of n, and the limit case of $n = 0$ will correspond to the original model,[10] i.e., ignoring the delay of drivers' response in sensing headway. The stability region decreases with the increase of n. This means that the traffic jams will appear easily when the drivers' delay in response increases, or when the sensitivity of drivers decreases. This phenomenon coincides with the real traffic.

On the basis of the nonlinear analysis, we obtain the propagation velocities c of the kink–antikink soliton solution from Eq.(31) for models A and B. It can be found that the propagation velocity $c_{\rm A}$ of model A is a constant, while the propagation velocity $c_{\rm B}$ of model B decreases with the increase of n which is shown in Table 1. This indicates that the jams are difficult to disperse when drivers have large delay of response, and the traffic will be in a terrible situation.

Table 1. The propagation velocity $c_{\rm B}$ in model B.

n	0	0.1	0.2	0.3	0.4	0.5
$c_{\rm B}$	27.00	26.60	26.27	26.00	25.79	25.6

6. Summary

We have proposed two lattice hydrodynamic models of traffic flow, which take into account the drivers' delay in sensing headway by giving a modified form of optimal velocity function. The traffic nature has been analysed by using the linear stability theory and the nonlinear analysis. We have derived the mKdV equations to describe the traffic jam near the critical points for models A and B respectively, and obtained the kink–antikink soliton solutions related to the traffic density waves. It has been shown that there exist critical points in the two models. The diagrams in the headway-sensitivity space with the neutral stability lines and the coexisting curves are given for different values of n, which denotes the proportion of drivers' delay in response to the total delay. It can be found that the stability regions decrease with the increase of n in each model, and the propagation velocity in model B decreases with the increase of n too. It indicates that the traffic jams will be easy to appear and difficult to disperse when the drivers' delay in response increases. The limit case of $n = 0$ corresponds to the original lattice version of the continuum models, and the results are identical. The study shows that the drivers' delay in response plays an important role in jamming transition.

Appendix

In this appendix, we give the expansions of each term in Eqs.(11) and (12) to fifth-order of ε:

$$\rho_j(t+\tau) = \rho_c + \varepsilon R + \varepsilon^2 b\tau\partial_X R + \varepsilon^3\frac{(b\tau)^2}{2}\partial_X^2 R + \varepsilon^4\frac{(b\tau)^3}{6}\partial_X^3 R + \varepsilon^4\tau\partial_T R + \varepsilon^5\frac{(b\tau)^4}{24}\partial_X^4 R + \varepsilon^5 b\tau^2\partial_T\partial_X R, \tag{A1}$$

$$\rho_j(t+2\tau) = \rho_c + \varepsilon R + \varepsilon^2 2b\tau\partial_X R + \varepsilon^3\frac{(2b\tau)^2}{2}\partial_X^2 R + \varepsilon^4\frac{(2b\tau)^3}{6}\partial_X^3 R + \varepsilon^4 2\tau\partial_T R + \varepsilon^5\frac{(2b\tau)^4}{24}\partial_X^4 R + \varepsilon^5 4b\tau^2\partial_T\partial_X R, \tag{A2}$$

$$\partial_t\rho_j(t+\tau) = \varepsilon^2 b\partial_X R + \varepsilon^3 b^2\tau\partial_X^2 R + \varepsilon^4\frac{b^3\tau^2}{2}\partial_X^3 R + \varepsilon^4\partial_T R + \varepsilon^5\frac{b^4\tau^3}{6}\partial_X^4 R + \varepsilon^5 2b\tau\partial_T\partial_X R, \tag{A3}$$

$$\rho_j(t-n\tau) = \rho_c + \varepsilon R - \varepsilon^2 bn\tau\partial_X R + \varepsilon^3\frac{(bn\tau)^2}{2}\partial_X^2 R - \varepsilon^4\frac{(bn\tau)^3}{6}\partial_X^3 R - \varepsilon^4 n\tau\partial_T R + \varepsilon^5\frac{(bn\tau)^4}{24}\partial_X^4 R + \varepsilon^5 bn^2\tau^2\partial_T\partial_X R, \tag{A4}$$

$$\rho_{j+1}(t) = \rho_c + \varepsilon R + \varepsilon^2\partial_X R + \frac{\varepsilon^3}{2}\partial_X^2 R + \frac{\varepsilon^4}{6}\partial_X^3 R + \frac{\varepsilon^5}{24}\partial_X^4 R, \tag{A5}$$

$$\begin{aligned}\rho_{j+1}(t-n\tau) = \rho_c &+ \varepsilon R + \varepsilon^2(1-bn\tau)\partial_X R + \varepsilon^3\left(1/2 - bn\tau + \frac{(bn\tau)^2}{2}\right)\partial_X^2 R \\ &+ \varepsilon^4\left[-n\tau\partial_T R + \left(\frac{1}{6} - \frac{bn\tau}{2} + \frac{(bn\tau)^2}{2} - \frac{(bn\tau)^3}{6}\right)\partial_X^3 R\right] \\ &+ \varepsilon^5\left[(-n\tau + bn^2\tau^2)\partial_T\partial_X R + \left(\frac{1}{24} - \frac{bn\tau}{6} + \frac{(bn\tau)^2}{4} - \frac{(bn\tau)^3}{6} + \frac{(bn\tau)^4}{24}\right)\partial_X^4 R\right].\end{aligned} \tag{A6}$$

We expand the optimal velocity function at the turning point:

$$V(\rho_j(t-n\tau)) = V(\rho_c) + V'(\rho_c)\cdot(\rho_j(t-n\tau)-\rho_c) + \frac{V'''(\rho_c)}{6}(\rho_j(t-n\tau)-\rho_c)^3, \tag{A7}$$

$$V(\rho_{j+1}(t-n\tau)) = V(\rho_c) + V'(\rho_c)\cdot(\rho_{j+1}(t-n\tau)-\rho_c) + \frac{V'''(\rho_c)}{6}(\rho_{j+1}(t-n\tau)-\rho_c)^3, \tag{A8}$$

$$\begin{aligned}V(\rho_{j+1}(t-n\tau)) - V(\rho_j(t-n\tau)) = V'(\rho_c)\cdot\Bigg\{&\varepsilon^2\partial_X R + \varepsilon^3(1/2-bn\tau)\partial_X^2 R + \varepsilon^4\left(\frac{1}{6} - \frac{bn\tau}{2} + \frac{(bn\tau)^2}{2}\right)\partial_X^3 R \\ &+ \varepsilon^5\left[-n\tau\partial_T\partial_X R + \left(\frac{1}{24} - \frac{bn\tau}{6} + \frac{(bn\tau)^2}{4} - \frac{(bn\tau)^3}{6}\right)\partial_X^4 R\right]\Bigg\} \\ &+ \frac{V'''(\rho_c)}{6}\left[\varepsilon^4\partial_X R^3 + \varepsilon^5(1/2-bn\tau)\partial_X^2 R^3\right].\end{aligned} \tag{A9}$$

We obtain Eq.(25) by inserting Eqs.(A3) and (A9) into Eq.(16), and obtain Eq.(26) by inserting Eqs.(A1), (A2) and (A9) into Eq.(17).

References

[1] Ge H X, Zhu H B and Dai S Q 2005 *Acta Phys. Sin.* **54** 4621 (in Chinese)

[2] Wang T, Gao Z Y and Zhao X M 2006 *Acta Phys. Sin.* **55** 634 (in Chinese)

[3] Ge H X, Dai S Q and Dong L Y 2008 *Chin. Phys.* B **17** 23

[4] Li K P, Gao Z Y and Mao B H 2007 *Chin. Phys.* **16** 359

[5] Xue Y 2002 *Chin. Phys.* **11** 1128

[6] Kurtze D A and Hong D C 1995 *Phys. Rev.* E **52** 218

[7] Kerner B S and Konhauser P 1993 *Phys. Rev.* E **48** 2335

[8] Komatsu T and Sasa S 1995 *Phys. Rev.* E **52** 5574

[9] Nagatani T 1998 *Physica* A **261** 599

[10] Nagatani T 1999 *Physica* A **264** 581

[11] Xue Y 2004 *Acta Phys. Sin.* **53** 25 (in Chinese)

[12] Ge H X, Dai S Q, Xue Y and Dong L Y 2005 *Phys. Rev.* E **71** 066119

[13] Nagatani T 1999 *Physica* A **265** 297

[14] Nagatani T 1999 *Physica* A **272** 592

[15] Bando M, Hasebe K, Nakayama A, Shibata A and Sugiyama Y 1995 *Phys. Rev.* E **51** 1035

[16] Whitham G B 1990 *Proc. R. Soc. London,* Ser. A **428** 49

[17] Bando M, Hasebe K, Nakanishi K and Nakayama A 1998 *Phys. Rev.* E **58** 5429

[18] Ge H X, Cheng R J and Dai S Q 2005 *Physica* A **357** 466